Electronic Supplementary Information

Effect of Boron Doping on Electrical Conductivity of Metallicity–Separated Single Walled Carbon Nanotube

Kazunori Fujisawa[1,2,*], Takuya Hayashi[1], Morinobu Endo[1,3], Mauricio Terrones[1,3,4] Jin Hee Kim[5,7] and Yoong Ahm Kim[6,7,*]

[1]Faculty of Engineering, Shinshu University, 4-17-1 Wakasato, Nagano, 380-8553, Japan.
[2]Department of Physics and Center for 2-dimensional and Layered Materials (2DLM), The Pennsylvania State University, University park, Pennsylvania 16802, United States.
[3]Institute of Carbon Science and Technology, Shinshu University, 4-17-1 Wakasato, Nagano, 380-8553, Japan.
[4]Department of Chemistry and Department of Materials Science and Engineering, The Pennsylvania State University, University Park, Pennsylvania 16802, United States.
[5]Faculty of Engineering, Chonnam National University, 77 Yongbong-ro, Buk-gu, Gwangju 61186, Republic of Korea.
[6]Department of Polymer Engineering, Graduate School, School of Polymer Science and Engineering & Department of Polymer Engineering, Graduate School, Chonnam National University, 77 Yongbong-ro, Buk-gu, Gwangju 61186, Republic of Korea.
[7]Institute for Biomedical Sciences, Interdisciplinary Cluster for Cutting Edge Research, Shinshu University, 3-1-1 Asahi, Matsumoto, Nagano, Japan.

Corresponding Authors
E-mail address: kuf15@psu.edu (K. Fujisawa), yak@jnu.ac.kr (Y.A. Kim)

Contents

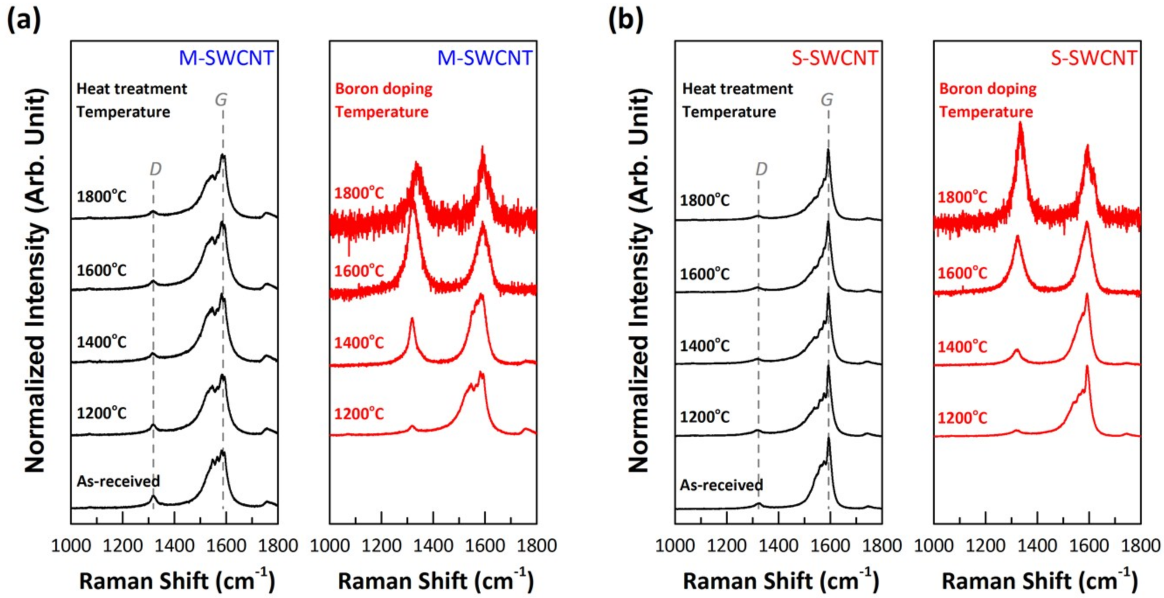

Figure S1. Raman spectra plotted with relative Raman intensity acquired from the metallic (a) and semiconducting (b) SWCNTs before and after heat-treatment, and boron doping.

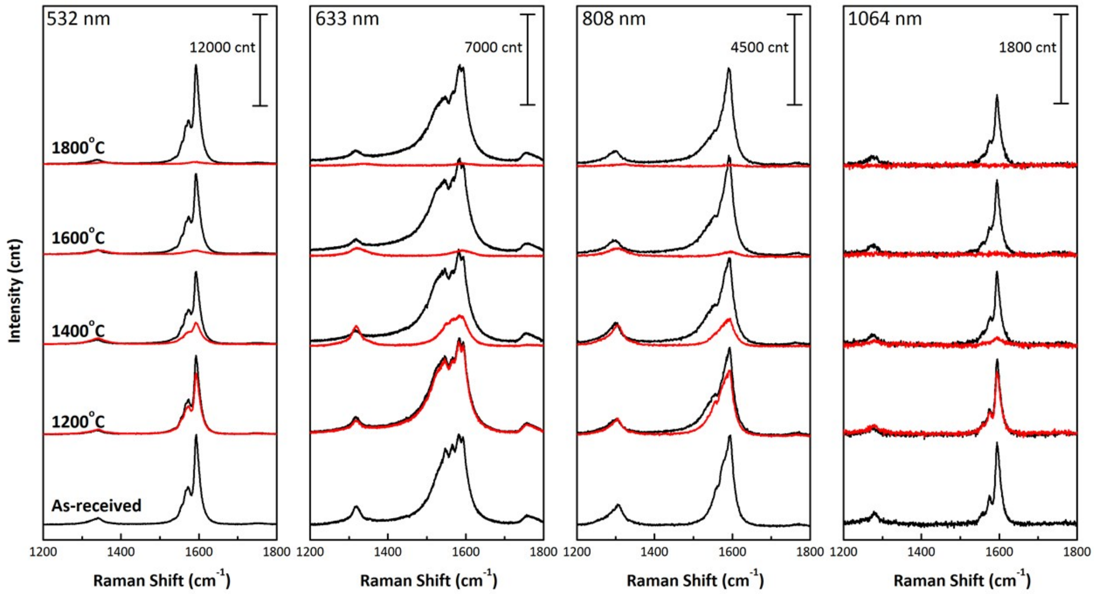

Figure S2. First order Raman spectra showing the D and G bands for the as-received, heat-treated (black line) and boron doped (red line) M-SWCNTs, taken with four different laser lines.

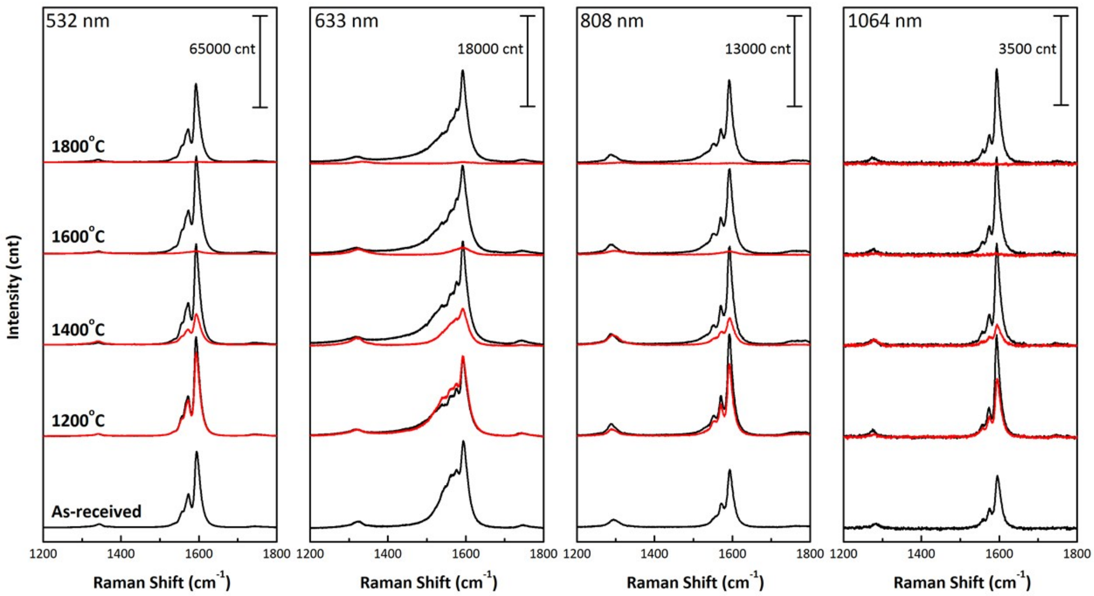

Figure S3. First order Raman spectra showing the D and G bands for the as-received, heat-treated (black line) and boron doped (red line) S-SWCNTs, taken with four different laser lines.

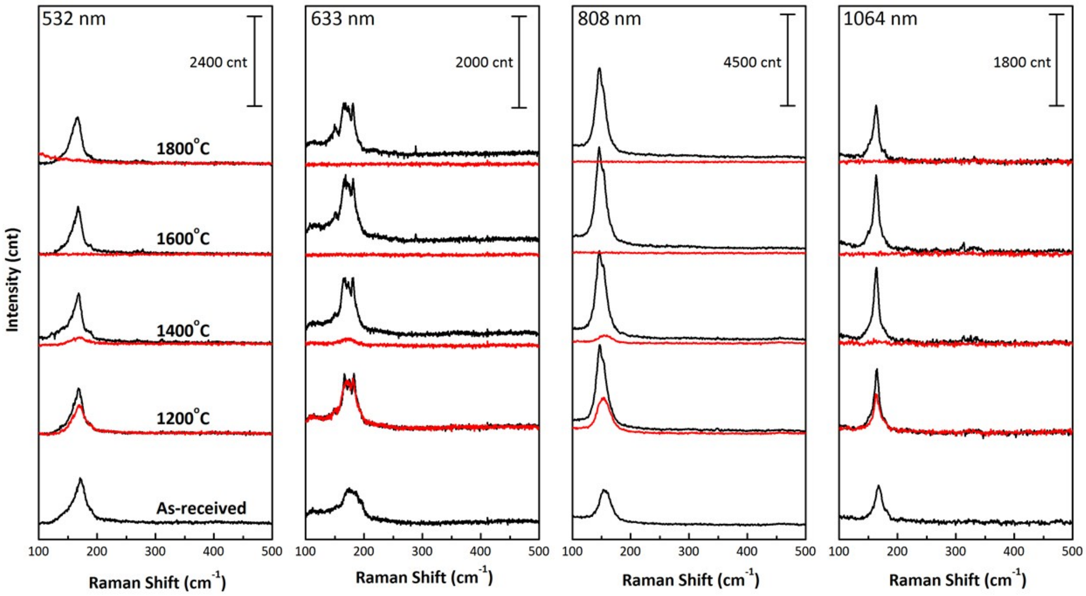

Figure S4. Low-frequency Raman spectra for the as-received, heat-treated (black line) and boron doped (red line) M-SWCNTs, taken with four different laser lines.

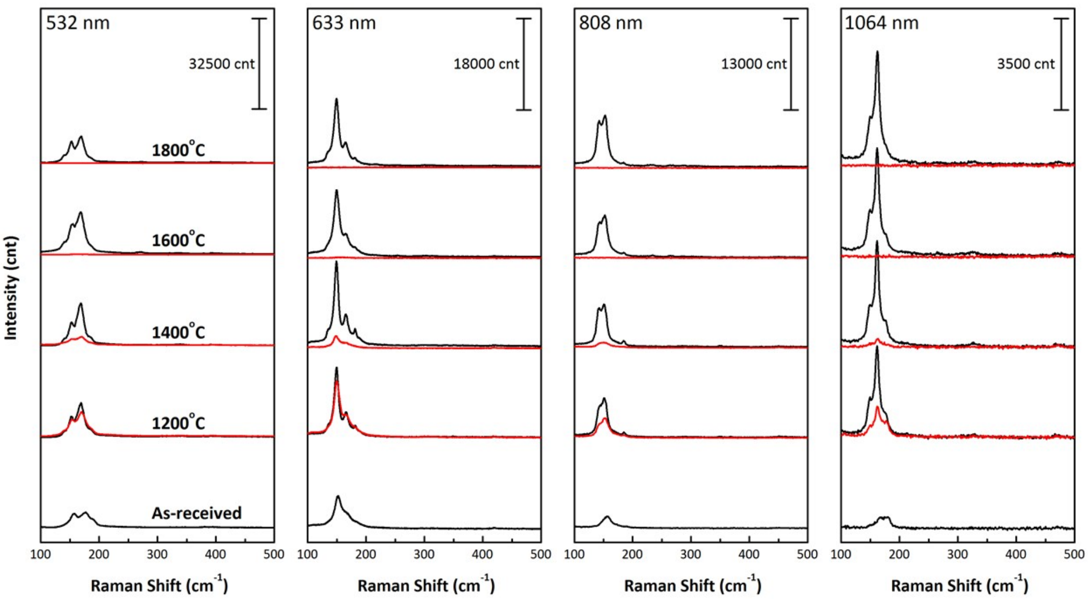

Figure S5. Low-frequency Raman spectra for the as-received, heat-treated (black line) and boron doped (red line) S-SWCNTs, taken with four different laser lines.

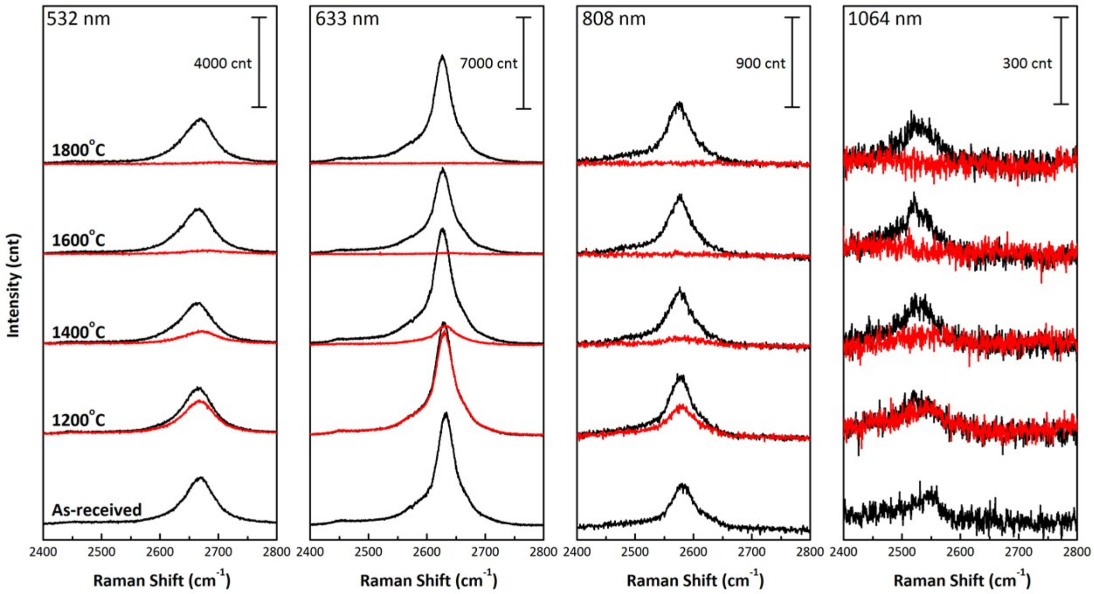

Figure S6. Second order Raman spectra for the as-received, heat-treated (black line) and boron doped (red line) M-SWCNTs, taken with four different laser lines.

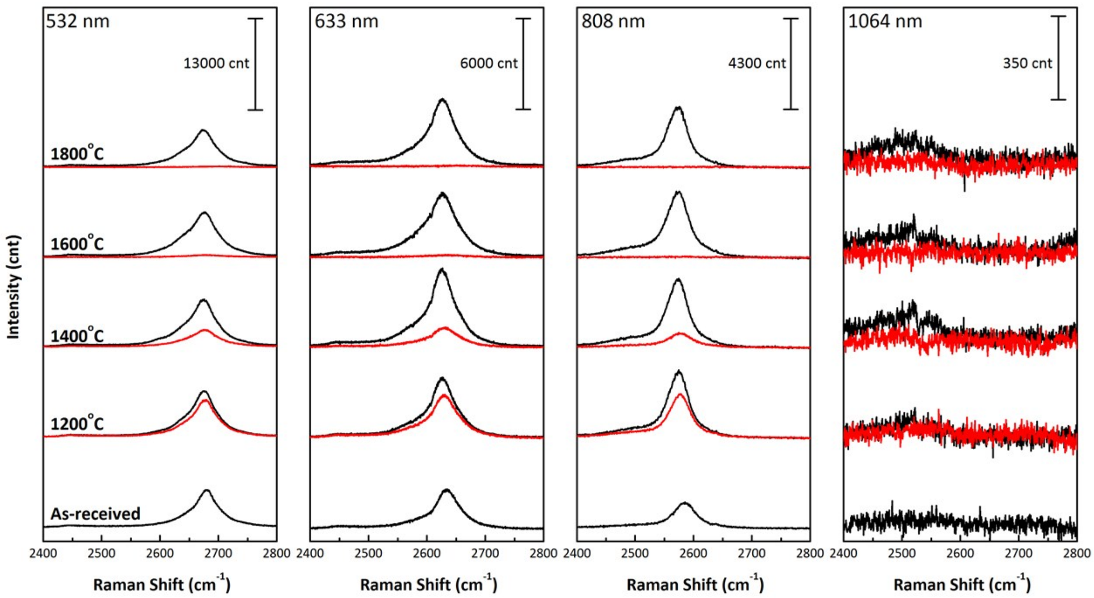

Figure S7. Second order Raman spectra for the as-received, heat-treated (black line) and boron doped (red line) S-SWCNTs, taken with four different laser lines.

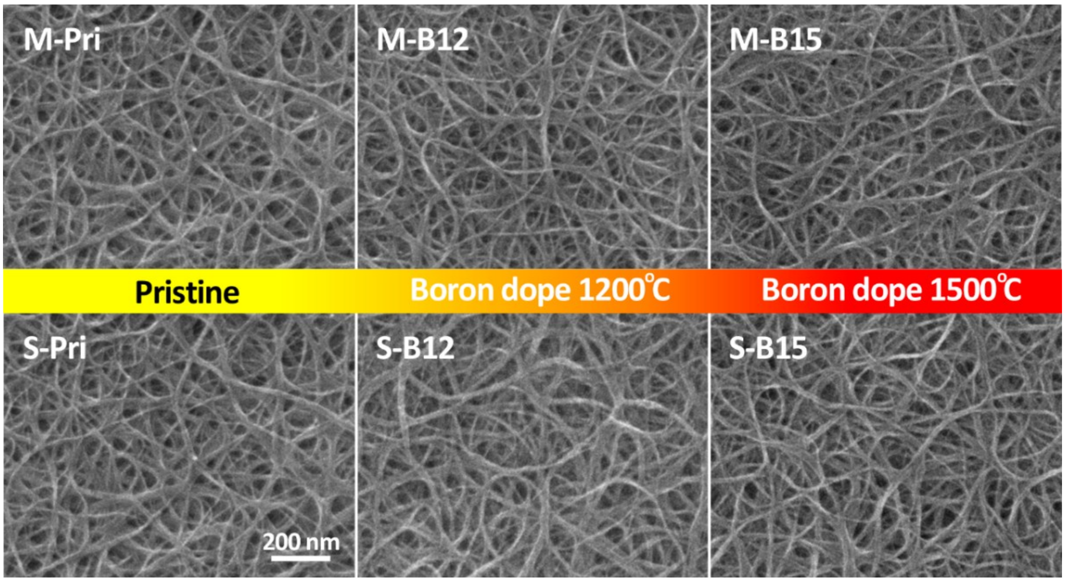

Figure S8. Scanning electron microscopic images of the pristine and boron doped M-SWCNTs and S-SWCNTs. There is no distinctive change in the surface morphology before and after boron doping.

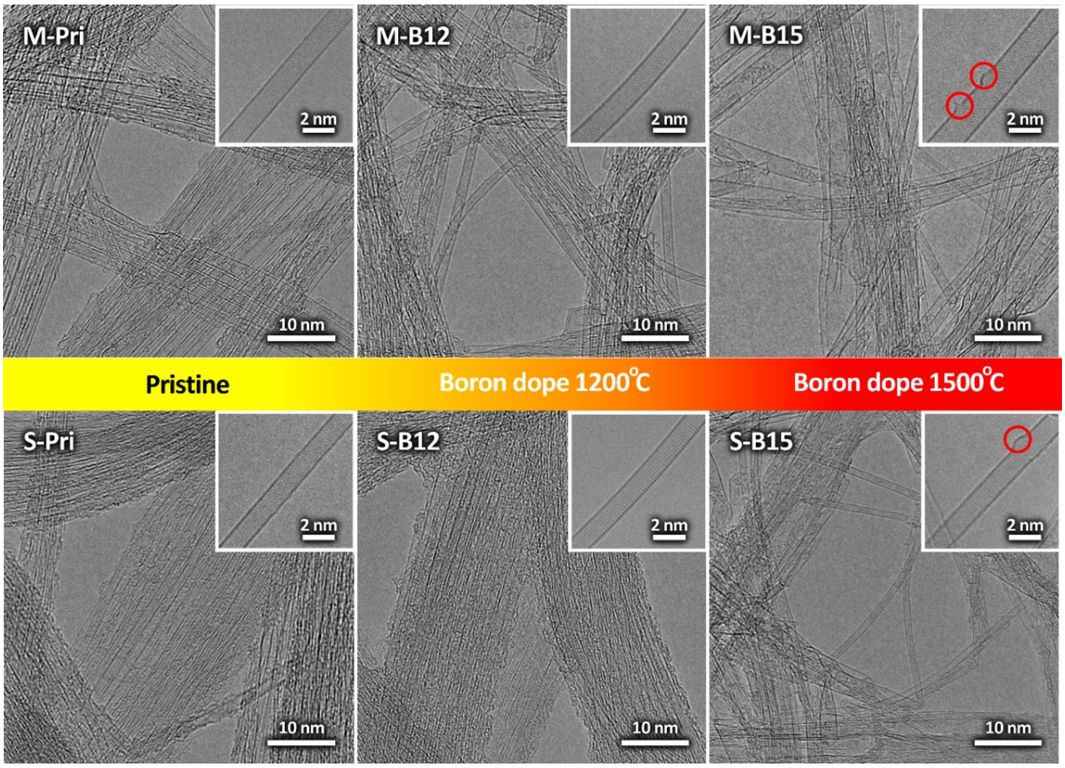

Figure S9. Aberration corrected high resolution transmission electron microscopic images of the pristine and boron doped M-SWCNTs and S-SWCNTs. The red circles in the inset for SWCNTs doped at 1500^{o}C indicate structural defect possibly caused by the incorporation of boron atoms and the formation of BC_3 domain.

Table S1 Chemical state of boron atom in boron doped carbon system.

Material	Precursor	Peak Position	Assignment	Reference
B-pyrocarbon [1]	Boron Chloride (BCl_3)	186.5	B Cluster	
		187.8	B_4C	
		188.8	BC_3	
		190.0	BC_2O	
		192.0	BCO_2	
		193.2	B_2O_3	
B-DWCNT [2]	Borane (BH_3)	191.4	BC_3	
B-SWCNT [3]	Triisopropyl Borate ($C_9H_{21}BO_3$)	187.0	Elemental Boron	Referring [2]
		190.0	BC_3 in Carbon	
		191.5-192.1	BC_3 in SWCNT	
		198.0	-	
		199.5	-	
B-Graphene [4]	Diborane (B_2H_6), Boron-stuffed Graphite	189.0	BC_3	Referring [2]
B-Graphene [5]	Boron Oixde (B_2O_3)	187.7	B_4C	Referring [2], [3]
		189.0	BC_3	
		190.4	BC_2O	
		191.9	BCO_2	
B-Graphene [6]	Boric Acid (H_3BO_3)	186.7	B_4C	Referring [4]
		187.1	Elemental Boron	
		190.6	BC_3	
B-Graphene [7]	Trimethylboron ($B(CH_3)_3$)	189.7	B-C	Referring [2], [3]
B-Graphene [8]	Phenylboronic Acid ($C_6H_7BO_2$)	190.9	BC_3	Referring [2]
B-Graphene/ Ni(111) [9]	Triethylborane ($C_6H_{15}B$)	187.4	BC_3	
B-MWCNT [10]	Triphenylborane ($C_{18}H_{15}B$)	186.5	B Cluster	Referring [1]
		187.5	B_4C	
		189.5	BC_3	
		191.0	BC_2O	
		192.3	BCO_2	
		193.0	B_2O_3	
B-MWCNT [11]	Triphenylborane ($C_{18}H_{15}B$)	186.6	B Cluster	Referring [1]
		187.6	B_4C	
		189.5	BC_3	
		191.0	BCN	
		191.4	BC_2O	
		192.5	BCO_2	
B-MWCNT [12]	Diborane (B_2H_6)	191.0	B-C	
B-DWCNT [13]	Triisopropyl Borate ($C_9H_{21}BO_3$)	187.9	B_4C	Referring [1]
		189.0	BC_3	
		190.0	BC_2O	
		192.0	BCO_2	
		193.2	B_2O_3	
B-SWCNT [14]	CoNiB Amorphous Alloy	190.1	B-C	
		192.6	B-O	
B-SWCNT [15]	Boron Oxide (B_2O_3)	191.5	BC_3	Referring [3]
		192.8	B_2O_3	
$C_{59}B$ [16]	Boron Nitide (BN), Boron Carbide (B_4C), Boron	188.8	BC_3	
		192.4	H_3BO_3, B_2O_3	

Table S2. Resistivity of the pristine and boron doped SWCNT sheets measured at 297 K.

I.D.	Resistivity at 297 K (Ω·cm)				
	Pristine	Boron doping temperature (^{o}C)			
		1200	1300	1400	1500
Metallic	3.02×10^{-4}	3.19×10^{-4}	1.07×10^{-3}	1.27×10^{-3}	1.36×10^{-3}
Un-separated	5.60×10^{-3}	3.58×10^{-3}	3.34×10^{-3}	3.11×10^{-3}	3.17×10^{-3}
Semiconducting	2.50×10^{-1}	1.79×10^{-2}	1.03×10^{-2}	8.16×10^{-3}	5.63×10^{-3}

Reference:

[1] S. Jacques, A. Guette, X. Bourrat, F. Langlais, C. Guimon, and C. Labrugere, Carbon N. Y. **34**, 1135 (1996).

[2] L. S. Panchakarla, A. Govindaraj, and C. N. R. Rao, ACS Nano **1**, 494 (2007).

[3] P. Ayala, W. Plank, A. Grüneis, E. I. Kauppinen, M. H. Rümmeli, H. Kuzmany, and T. Pichler, J. Mater. Chem. **18**, 5676 (2008).

[4] L. S. Panchakarla, K. S. Subrahmanyam, S. K. Saha, A. Govindaraj, H. R. Krishnamurthy, U. V. Waghmare, and C. N. R. Rao, Adv. Mater. **21**, NA (2009).

[5] Z.-H. Sheng, H.-L. Gao, W.-J. Bao, F.-B. Wang, and X.-H. Xia, J. Mater. Chem. **22**, 390 (2012).

[6] T. Wu, H. Shen, L. Sun, B. Cheng, B. Liu, and J. Shen, New J. Chem. **36**, 1385 (2012).

[7] Y.-B. Tang, L.-C. Yin, Y. Yang, X.-H. Bo, Y.-L. Cao, H.-E. Wang, W.-J. Zhang, I. Bello, S.-T. Lee, H.-M. Cheng, and C.-S. Lee, ACS Nano **6**, 1970 (2012).

[8] H. Wang, Y. Zhou, D. Wu, L. Liao, S. Zhao, H. Peng, and Z. Liu, Small **9**, 1316 (2013).

[9] W. Zhao, J. Gebhardt, K. Gotterbarm, O. Höfert, C. Gleichweit, C. Papp, A. Görling, and H.-P. Steinrück, J. Phys. Condens. Matter **25**, 445002 (2013).

[10] L. Yang, S. Jiang, Y. Zhao, L. Zhu, S. Chen, X. Wang, Q. Wu, J. Ma, Y. Ma, and Z. Hu, Angew. Chemie **123**, 7270 (2011).

[11] Y. Zhao, L. Yang, S. Chen, X. Wang, Y. Ma, Q. Wu, Y. Jiang, W. Qian, and Z. Hu, (2013).

[12] R. B. Sharma, D. J. Late, D. S. Joag, A. Govindaraj, and C. N. R. Rao, Chem. Phys. Lett. **428**, 102 (2006).

[13] S. C. Lyu, J. H. Han, K. W. Shin, and J. H. Sok, Carbon N. Y. **49**, 1532 (2011).

[14] B. Wang, Y. Ma, Y. Wu, N. Li, Y. Huang, and Y. Chen, Carbon N. Y. **47**, 2112 (2009).

[15] B. Anand, R. Podila, P. Ayala, L. Oliveira, R. Philip, S. S. Sankara Sai, A. A. Zakhidov, and A. M. Rao, Nanoscale **5**, 7271 (2013).

[16] H.-J. Muhr, R. Nesper, B. Schnyder, and R. Kötz, Chem. Phys. Lett. **249**, 399 (1996).